Long-wave transverse instability of interfacial gravity–capillary solitary waves in a two-layer potential flow in deep water

Boguk Kim

Abstract Interfacial gravity–capillary plane solitary waves, driven by the gravitational force in the presence of interfacial tension in a two-layer deep-water potential flow, bifurcate in the form of wavepackets with a non-zero carrier wavenumber at which the phase speed is minimized. A stability property for the interfacial gravity–capillary plane solitary waves is presented within the framework of the full Euler equations: according to a linear stability analysis based on the perturbation method, such waves are unstable under weak and long-wave disturbances in the transverse direction to the dominant wave propagation. An instability criterion is verified that the total mechanical energy of the solitary waves is a decreasing function of the solitary wavespeed, owing to the fact that the speed of the bifurcating solitary wavepackets is less than the minimum of the phase speed. This result is consistent with an earlier study on the transverse instability of the longitudinally stable interfacial gravity–capillary solitary waves from the Benjamin model equation for weakly nonlinear long interfacial elevations (Kim and Akylas, J Fluid Mech 557:237–256, 2006). The analysis is also applicable to other interfacial gravity–capillary solitary waves that may bifurcate below the minimum of the phase speed, regardless of any restrictions on fluid depths in two-layer potential flows.

Keywords Dispersive fluid wave systems · Euler equations · Solitary waves · Three-dimensional flow · Total mechanical energy

1 Introduction

We consider two immiscible fluid layers, in which the lighter layer with a constant fluid density ρ_2 is laid over the heavier one with ρ_1 ($\rho_1 > \rho_2$). One of the layers of a finite thickness h is located on the top or on the bottom of the fluid system, bounded by a flat horizontal rigid wall. The depth of the other layer is much greater than h or possibly infinite. It is assumed that the boundary friction, if any, is negligible, so that the flow is irrotational.

In this physical setting, a line of studies has been developed on internal stationary waves moving along the interface between two fluid layers, beginning with T. B. Benjamin's interpretation of the dispersion relation. He predicted the existence of solitary waves in the small-amplitude and long-wave limit in the presence of interfacial

B. Kim (✉)
Centre de Mathématiques et de Leurs Applications, École Normale Supérieure de Cachan, CNRS UMR 8536,
61 Avenue du Président Wilson, 94235 Cachan Cedex, France
e-mail: boguk.kim@cmla.ens-cachan.fr

tension [1]. Internal stationary waves driven only by the gravitational force, not considering interfacial tension, are described in his earlier work [2].

The generation mechanism of gravity–capillary solitary waves has been identified as bifurcation in the form of wavepackets with a specific carrier wavenumber at which the linear phase speed is minimized [3–5]. At the carrier wavenumber, the component of the group velocity in the direction of phase propagation is equal to the phase speed: for plane wavepackets, in particular, the group velocity is the same as the phase speed. The envelope of wavepackets for the primary harmonic is governed by the nonlinear Schrödinger equation when the spectral bandwidth is narrow enough so as to be comparable to the small-wave-amplitude scale in the order of magnitude. Such a bifurcation scenario is now commonly accepted for either surface or interfacial solitary waves in potential flow systems. In the presence of surface or interfacial tension, together with the gravitational acceleration, the bifurcation point is found at a nonzero wavenumber.

The steady profiles of surface gravity–capillary solitary-wave solutions were computed from the full Euler equations in [6,7] earlier than the discovery of the above generation mechanism of gravity–capillary solitary waves. For the interfacial counterparts of a two-layer potential flow in finite depth, a numerical study was performed later involving the full Euler equations [8,9]. The weakly nonlinear long-wave version from the Benjamin model equation for interfacial gravity–capillary solitary waves was done by using numerical continuation in [10], where the steady model equation is parameterized by a speed-related parameter ranging from 0 to 1. The stability properties of such gravity–capillary solitary waves under disturbances along the same direction of the solitary-wave propagation, referred to as 'longitudinal stability', were throughly investigated for the surface solitary waves and for the interfacial ones, in [11] and [12] respectively, by Calvo and Akylas.

In contrast to the longitudinal stability, 'transverse stability' properties for the longitudinally stable gravity–capillary solitary waves under disturbances moving in the perpendicular horizontal direction from the solitary-wave propagation were studied later (see [13] for the use of the same terminology). For interfacial gravity–capillary waves, long-wave transverse dispersion was verified to be the well-known Kadomtsev–Petviashvili-I (KP-I) type in the context of the two-dimensional Benjamin (2-DB) model equation in [14]. In it, long-wave weak disturbances are assumed to propagate in arbitrary oblique directions, which can be transformed into perturbations only in the transverse direction to the solitary wave propagation but parallel to the fluid interface. And then, the long-wave transverse instability of surface gravity–capillary solitary waves was verified for the full Euler equations in [15] by the authors of [14].

The key idea in deriving the long-wave transverse instability criterion applied for both the weakly nonlinear long-wave interfacial solitary waves and the surface gravity–capillary solitary waves, demonstrated in [14,15], is essentially the same. The instability growth rate at the initial stage when long-wave transverse disturbances start to develop is expressed in terms of the underlying solitary-wave solutions. From the associated nonlinear eigenvalue problem, the eigenvalue and the associated eigenfunction correspond to the instability growth rate and the specific transverse perturbation, respectively. A useful sufficient condition for long-wave transverse disturbances to grow exponentially is that the total mechanical energy $\mathcal{E}$ of the solitary waves should be a decreasing function of the wavespeed V. In fact,

$$\frac{\partial \mathcal{E}}{\partial V} < 0 \tag{1.1}$$

should be always valid for the gravity–capillary solitary waves under consideration near the bifurcation point if they bifurcate *below* the minimum of the linear phase speed. It is because their total mechanical energy increases but their wavespeed decreases as they are farther away below from the bifurcation point.

From the previous results for gravity–capillary solitary waves, it seems to be evident that interfacial gravity–capillary solitary waves share many stability properties with surface gravity–capillary solitary waves. Moreover, the existence of interfacial gravity–capillary solitary waves may not necessarily require extra assumptions, for instance, such as weak nonlinearity or long-waveness that are assumed for the Benjamin model equation. Accordingly, the main objective of the present study is to obtain a generalized result for the long-wave transverse instability of interfacial gravity–capillary solitary waves within the framework of the full Euler equations, not only from model equations, in a consistent manner that was employed for the long-wave transverse instability of the surface
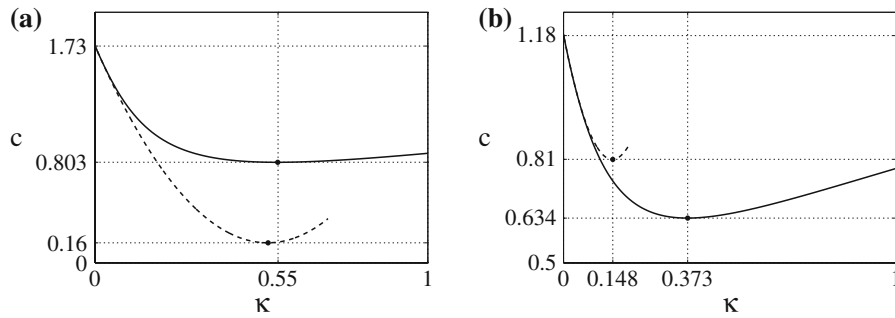
Fig. 1 The linear dispersion relation of the full Euler equations for interfacial gravity–capillary waves when the finite depth layer is located on the bottom of a two-fluid potential flow system (2.9) (*solid*) and its long-wave approximation (2.11) (*dotted*) are compared by plotting wavenumber κ versus phase speed $c = \omega/\kappa$. The two nondimensional parameters $R = \rho_2/\rho_1$ and $H = h\sqrt{(\rho_1 g)/T}$ are defined. (**a**) corresponds to the dispersion relation for monochromatic waves that propagate on the interface of an infinitely deep m-xylene layer on the 4.6 cm-deep water for $R = 0.7$ and $H = 10$: the critical wavenumbers are found in the region where the long-wave approximation fails so that the critical phase speeds at the minimum points of the phase speeds differ significantly each other. (**b**) represents the dispersion relation for the infinitely deep benzene on the 3.5 cm-deep water for $R = 0.86$ and $H = 10$: there is a huge gap between the two critical wavenumbers at the bifurcation points. The values of the physical parameters are found in [1,12]. $H \gg 1$ implies the weak interfacial tension regime

gravity–capillary solitary waves in [15]. In other words, we aim to make similar long-wave transverse instability statements in other parameter regimes, as well, especially where interfacial tension is weak.

In general, the long-waveness assumption states that the principal components among the Fourier modes of waves are achieved only when the wavenumber is close to zero. According to the original consideration by Benjamin [1], the long-waveness assumption is justified by the condition

$$W = \sqrt{\frac{T}{\delta\rho g h^2}} \gg 1, \tag{1.2}$$

where T is the interfacial tension coefficient, $\delta\rho = \rho_1 - \rho_2$ is the density difference, and g is the gravitational acceleration. This condition (1.2) has been taken for granted by some later authors writing on interfacial gravity–capillary solitary waves in deep water [12,14]. If the wavelength scale is nondimensionalized by $\sqrt{T/(\rho_1 g)}$ instead of h, however, then it turns out to be equivalent to using

$$1 - R = 1 - \frac{\rho_2}{\rho_1} = \frac{\delta\rho}{\rho_1} \ll 1 \tag{1.3}$$

in order to validate the same long-waveness assumption (see Appendix for the reasoning). This *close-density condition* (1.3) is assumed in [16] to derive the two-dimensional Benjamin model equation for weakly nonlinear and long interfacial elevation. As is shown in Fig. 1, there are apparent discrepancies between the original dispersion relation and its long-wave limit, either in the critical wavenumbers or in the minimum phase speeds, for a few selected physical parameters that represent weak interfacial tension regimes.

According to other related studies on transverse instability analysis for solitary waves that are found either on the surface or on the interface of fluids, with or without the surface or the interfacial tension [13–15,17,18], transverse instability occurs if the same criterion (1.1) is satisfied. This argument on transverse instability should be valid regardless of the configuration of a finite-depth layer whether it is on the top or on the bottom of the whole fluid system.

A fascinating aspect of transverse instability for gravity–capillary solitary waves is that it is considered as a sign of the occurrence of interesting dimension-breaking phenomena in three-dimensional surface or interfacial wave dynamics. It is thought that the long-wave transverse instability of two-dimensional (also referred to as plane or line) gravity–capillary solitary waves is closely related to the existence of lump-type solitary waves. Referred to as 'gravity–capillary lumps', as recently studied in [14,19–24], they follow the same bifurcation scenario as that of the two-dimensional counterpart in the same physical condition described in this study. In [14], preceded by

[19–22] for the surface wave counterparts, the numerical profiles for the steady solutions of interfacial gravity–capillary lumps in deep water were computed from the elliptic–elliptic Benney–Roskes–Davey–Stewartson (BRDS) equations that were extended in [25,26] by including the surface tension effect in three dimensions. The associated unsteady numerical results in the context of the full Euler equations for interfacial gravity–capillary waves have been obtained in [27,28].

It was shown that the lumps are dynamically generated from the plane solitary waves induced by weak and long-wave transverse disturbances for interfacial gravity–capillary solitary waves in [14]. For surface gravity–capillary solitary waves, Akers and Milewski demonstrated similar results from their model equation in [23]. A rigorous eigenvalue problem for the stability of depression gravity–capillary lumps was studied in [24] in the context of the fifth-order KP model equation for surface gravity–capillary waves, concluding that depression gravity–capillary lumps beyond a certain critical threshold in their amplitude or steepness are stable under three dimensional weak disturbances. A consistent stability statement of steady surface gravity–capillary lumps was mentioned in [23] based on the energy plots with respect to the wavespeed for steady solitary-wave lump solutions. Their solid justifications on the three-dimensional stability of the gravity–capillary lumps give mutual credence to the long-wave transverse instability of gravity–capillary solitary waves that have been investigated through all of the prior works as well as the current study.

2 Formulation

2.1 Nondimensionalization

Let us nondimensionalize the wavelength scale by $\sqrt{T/(\rho_1 g)}$ and the time scale by $\{T/(\rho_1 g^3)\}^{1/4}$. It follows that the potential functions in both fluid layers are nondimensionalized by $\{T^3/(\rho_1^3 g)\}^{1/4}$. This nondimensionalization allows a long-wave approximation to be possible if the close-density condition (1.3) is satisfied. In many other instances, the length scale can be nondimensionalized by h (with the same time scale by $\{T/(\rho_1 g^3)\}^{1/4}$), for which the potential functions are to be scaled by $h^2(\rho_1 g^3/T)^{1/4}$. For any choices, the resulting nondimensional equations should be congruent up to an appropriate scaling.

The nondimensional Euler equations for a two-layer potential flow, when the finite-depth layer of the thickness h is on the bottom of the fluid system, read as follows:

$$\nabla^2 \phi_1 = 0 \quad \text{for} \ -H < z < \eta(x, y, t), \tag{2.1a}$$

$$\nabla^2 \phi_2 = 0 \quad \text{for} \ \eta(x, y, t) < z < +\infty, \tag{2.1b}$$

with the boundary and far field conditions

$$\phi_{1,z} = 0 \quad \text{at} \ z = -H, \tag{2.2a}$$

$$\phi_{1,x} \to 0 \quad \text{as} \ x \to \pm\infty, \tag{2.2b}$$

$$\phi_{1,y} \to 0 \quad \text{as} \ y \to \pm\infty, \tag{2.2c}$$

$$\phi_{2,z} \to 0 \quad \text{as} \ z \to +\infty, \tag{2.2d}$$

$$\phi_{2,x} \to 0 \quad \text{as} \ x \to \pm\infty, \tag{2.2e}$$

$$\phi_{2,y} \to 0 \quad \text{as} \ y \to \pm\infty, \tag{2.2f}$$

where

$$\nabla^2 \equiv \frac{\partial^2}{\partial x^2} + \frac{\partial^2}{\partial y^2} + \frac{\partial^2}{\partial z^2} \tag{2.3}$$

for $\phi_1(x, y, z, t)$ and $\phi_2(x, y, z, t)$. As customary, x and y are the horizontal variables, z is the vertical variable in the direction of the gravitational acceleration, and t is the time variable. The nondimensional parameter H, the

depth of the finite-depth fluid, is defined by

$$H = h\sqrt{\frac{\rho_1 g}{T}}. \tag{2.4}$$

This nondimensional variable H measures the ratio between the gravitational force exerting on the heavier fluid and the strength of the interfacial tension.

When the finite-depth layer is on the top of the fluid system, on the other hand, the nondimensional system of equations is given by

$$\nabla^2 \phi_1 = 0 \quad \text{for} \quad -\infty < z < \eta(x, y, t), \tag{2.5a}$$
$$\nabla^2 \phi_2 = 0 \quad \text{for} \quad \eta(x, y, t) < z < H, \tag{2.5b}$$

with the boundary and far field conditions

$$\phi_{1,z} \to 0 \quad \text{as} \quad z \to -\infty, \tag{2.6a}$$
$$\phi_{1,x} \to 0 \quad \text{as} \quad x \to \pm\infty, \tag{2.6b}$$
$$\phi_{1,y} \to 0 \quad \text{as} \quad y \to \pm\infty, \tag{2.6c}$$
$$\phi_{2,z} = 0 \quad \text{at} \quad z = H, \tag{2.6d}$$
$$\phi_{2,x} \to 0 \quad \text{as} \quad x \to \pm\infty, \tag{2.6e}$$
$$\phi_{2,y} \to 0 \quad \text{as} \quad y \to \pm\infty, \tag{2.6f}$$

For either physical configuration, the interfacial conditions on the fluid interface $z = \eta(x, y, t)$ are the same. The two kinematic boundary conditions are nondimensionalized to be

$$\eta_t + \phi_{1,x}\eta_x + \phi_{1,y}\eta_y = \phi_{1,z}, \tag{2.7a}$$
$$\eta_t + \phi_{2,x}\eta_x + \phi_{2,y}\eta_y = \phi_{2,z}. \tag{2.7b}$$

The nondimensional dynamic boundary condition is written by

$$\phi_{1,t} + \frac{1}{2}\left(\phi_{1,x}^2 + \phi_{1,y}^2 + \phi_{1,z}^2\right) - R\left\{\phi_{2,t} + \frac{1}{2}\left(\phi_{2,x}^2 + \phi_{2,y}^2 + \phi_{2,z}^2\right)\right\}$$
$$+ (1-R)\eta - \left\{\left(\frac{\eta_x}{\sqrt{1 + \eta_x^2 + \eta_y^2}}\right)_x + \left(\frac{\eta_y}{\sqrt{1 + \eta_x^2 + \eta_y^2}}\right)_y\right\} = 0. \tag{2.8}$$

Note that the interfacial tension coefficient is normalized with our choice of the length and time scales (the lower alphabetical and Greek subscripts represent partial differentiations with respect to the subscript variables).

2.2 Dispersion relation

In dispersive wave systems, the linear dynamics of infinitesimally small amplitude waves is completely determined by the dispersion relation. In addition, the dispersion relation contains information on the bifurcation scenario of solitary waves.

When the finite-depth layer is on the bottom of the fluid system, the dispersion relation corresponding to (2.1), (2.2a), (2.7), and (2.8) is

$$\omega^2 = \frac{(1-R)\kappa + \kappa^3}{R + \coth(\kappa H)}, \tag{2.9}$$

where

$$\kappa = \sqrt{k^2 + l^2}, \tag{2.10}$$

assuming that monochromatic waves along the fluid interface take the form of $e^{i(kx+ly-\omega t)}$. In the long-wave limit as $\kappa \to 0$, (2.9) is approximated by

$$\omega \sim \sqrt{(1-R)\,H\kappa} \left\{ 1 - \frac{1}{2}RH\kappa + \frac{1}{2}\left(\frac{1}{1-R} - \frac{H^2}{3} + \frac{3R^2H^2}{4} \right)\kappa^2 \right\}. \tag{2.11}$$

When the finite-depth layer is on the top of the fluid system, on the other hand, the dispersion relation corresponding to (2.5)–(2.8) becomes

$$\omega^2 = \frac{(1-R)\,\kappa + \kappa^3}{1 + R\coth(\kappa H)}, \tag{2.12}$$

and the associated long-wave approximation is

$$\omega \sim \sqrt{\frac{(1-R)\,H}{R}}\kappa \left\{ 1 - \frac{H}{2R}\kappa + \frac{1}{2}\left(\frac{1}{1-R} - \frac{H^2}{3} + \frac{3H^2}{4R^2} \right)\kappa^2 \right\}. \tag{2.13}$$

In the following sections, most discussions are presented assuming that the finite-depth layer is on the bottom of the fluid system. For the other physical configuration, only minor modifications are needed to reach an equivalent set of results.

2.3 Linearized system for transverse perturbations to interfacial gravity–capillary plane solitary waves in deep water

A perturbation method was used to verify the long-wave transverse instability criterion for surface gravity solitary waves in [17], for surface gravity–capillary solitary waves in [15], and for interfacial gravity solitary waves in [13]. In this section, a method essentially identical to the previous ones is first attempted in the framework of a two-layer potential flow system in deep water with the presence of both the gravitational acceleration and the interfacial tension.

Suppose that

$$\bar{\eta}(\xi) = \bar{\eta}(x - Vt) \tag{2.14}$$

is a plane solitary-wave solution for the interfacial elevation moving in the x-direction only. The corresponding solitary-wave solutions for the two potential functions are denoted by

$$\bar{\phi}_1(\xi, z) = \bar{\phi}_1(x - Vt, z), \tag{2.15a}$$
$$\bar{\phi}_2(\xi, z) = \bar{\phi}_2(x - Vt, z), \tag{2.15b}$$

in the lower and upper layers, respectively (the solitary-wave solutions are denoted by the variables with the bar on the top). The transversely perturbed solutions in the y-direction are

$$\eta(x, y, t) = \bar{\eta}(\xi) + \hat{\eta}(\xi)e^{i\mu y + \lambda t}, \tag{2.16a}$$
$$\phi_1(x, y, z, t) = \bar{\phi}_1(\xi, z) + \hat{\phi}_1(\xi, z)e^{i\mu y + \lambda t}, \tag{2.16b}$$
$$\phi_2(x, y, z, t) = \bar{\phi}_2(\xi, z) + \hat{\phi}_2(\xi, z)e^{i\mu y + \lambda t}, \tag{2.16c}$$

where λ is defined by the instability growth rate. Here it is assumed that

$$\left|\hat{\phi}_1\right| \ll |\bar{\phi}_1|, \quad \left|\hat{\phi}_2\right| \ll |\bar{\phi}_2|, \quad |\hat{\eta}| \ll |\bar{\eta}|. \tag{2.17}$$

The linearized system of equations for the perturbed waves then becomes

$$\bar{\nabla}^2 \hat{\phi}_1 = \mu^2 \hat{\phi}_1 \quad \text{for } -H < z < \bar{\eta}, \tag{2.18a}$$
$$\bar{\nabla}^2 \hat{\phi}_2 = \mu^2 \hat{\phi}_2 \quad \text{for } \bar{\eta} < z < +\infty, \tag{2.18b}$$

where

$$\bar{\nabla}^2 \equiv \frac{\partial^2}{\partial \xi^2} + \frac{\partial^2}{\partial z^2}, \tag{2.19}$$

with the bottom boundary condition

$$\hat{\phi}_{1,z} = 0 \quad \text{at} \quad z = -H, \tag{2.20}$$

and the far field conditions

$$\hat{\phi}_{2,z} \to 0 \quad \text{as} \quad z \to +\infty, \tag{2.21a}$$
$$\hat{\phi}_{1,\xi} \to 0 \quad \text{as} \quad \xi \to \pm\infty, \tag{2.21b}$$
$$\hat{\phi}_{2,\xi} \to 0 \quad \text{as} \quad \xi \to \pm\infty. \tag{2.21c}$$

The kinematic and dynamic conditions at the interface $z = \bar{\eta}(\xi)$ are

$$\mathcal{L}_1\left(\hat{\phi}_1, \hat{\phi}_2, \hat{\eta}\right) = -\lambda\hat{\eta}, \tag{2.22a}$$

$$\mathcal{L}_2\left(\hat{\phi}_1, \hat{\phi}_2, \hat{\eta}\right) = -\lambda\hat{\eta}, \tag{2.22b}$$

$$\mathcal{L}_3\left(\hat{\phi}_1, \hat{\phi}_2, \hat{\eta}\right) = -\lambda\left(\hat{\phi}_1 - R\hat{\phi}_2\right) - \mu^2\frac{\hat{\eta}}{\sqrt{1 + \bar{\eta}_\xi^2}}, \tag{2.22c}$$

where

$$\mathcal{L}_1 \equiv -\sqrt{1 + \bar{\eta}_\xi^2}\frac{\partial}{\partial\vec{n}_1}\hat{\phi}_1 + \left\{\frac{\mathrm{d}}{\mathrm{d}\xi}\bar{\phi}_{1,\xi} + \left(-V + \bar{\phi}_{1,\xi}\right)\frac{\mathrm{d}}{\mathrm{d}\xi}\right\}\hat{\eta}, \tag{2.23a}$$

$$\mathcal{L}_2 \equiv \sqrt{1 + \bar{\eta}_\xi^2}\frac{\partial}{\partial\vec{n}_2}\hat{\phi}_2 + \left\{\frac{\mathrm{d}}{\mathrm{d}\xi}\bar{\phi}_{2,\xi} + \left(-V + \bar{\phi}_{2,\xi}\right)\frac{\mathrm{d}}{\mathrm{d}\xi}\right\}\hat{\eta}, \tag{2.23b}$$

$$\mathcal{L}_3 \equiv \left(-V + \bar{\phi}_{1,\xi}\right)\frac{\mathrm{d}}{\mathrm{d}\xi}\hat{\phi}_1 - R\left(-V + \bar{\phi}_{2,\xi}\right)\frac{\mathrm{d}}{\mathrm{d}\xi}\hat{\phi}_2 + \sqrt{1 + \bar{\eta}_\xi^2}$$

$$\times \left\{\left(-V + \bar{\phi}_{1,\xi}\right)\frac{\partial}{\partial\vec{n}_1}\bar{\phi}_{1,\xi} + R\left(-V + \bar{\phi}_{2,\xi}\right)\frac{\partial}{\partial\vec{n}_2}\bar{\phi}_{2,\xi}\right\}\hat{\eta} + (1 - R)\,\hat{\eta} - \left\{\frac{\hat{\eta}_\xi}{\left(1 + \bar{\eta}_\xi^2\right)^{3/2}}\right\}_\xi. \tag{2.23c}$$

As usual, $\frac{\mathrm{d}}{\mathrm{d}\xi}$ is the directional derivative in the ξ-direction along the fluid interface $z = \bar{\eta}(\xi)$, defined by

$$\frac{\mathrm{d}}{\mathrm{d}\xi} \equiv \frac{\partial}{\partial\xi} + \bar{\eta}_\xi\frac{\partial}{\partial z}. \tag{2.24}$$

The normal vectors at the interface $z = \bar{\eta}(\xi)$ are defined by

$$\vec{n}_1 \equiv \frac{1}{\sqrt{1 + \bar{\eta}_\xi^2}}\left(-\bar{\eta}_\xi, 1\right) \equiv -\vec{n}_2. \tag{2.25}$$

Hence, the associated normal derivatives are given by

$$\frac{\partial}{\partial\vec{n}_1} \equiv -\frac{\bar{\eta}_\xi}{\sqrt{1 + \bar{\eta}_\xi^2}}\frac{\partial}{\partial\xi} + \frac{1}{\sqrt{1 + \bar{\eta}_\xi^2}}\frac{\partial}{\partial z} \equiv -\frac{\partial}{\partial\vec{n}_2}. \tag{2.26}$$

Here $\vec{n}_1$ and $\vec{n}_2$ are the outward normal vectors on the fluid interface $z = \bar{\eta}(\xi)$ with respect to the lower and the upper layers, respectively. For the above derivation, we use the fact that

$$\bar{\nabla}^2\bar{\phi}_1 = 0 \quad \text{for} \quad -H < z < \bar{\eta}, \tag{2.27a}$$
$$\bar{\nabla}^2\bar{\phi}_2 = 0 \quad \text{for} \quad \bar{\eta} < z < +\infty. \tag{2.27b}$$

2.4 Long-wave perturbation expansion

Under the assumption of long-wave disturbances

$$|\mu| \ll 1, \tag{2.28}$$

the perturbed solutions are expanded in the small parameter μ as follows:

$$\hat{\phi}_1 = \hat{\phi}_1^{(0)} + \mu\hat{\phi}_1^{(1)} + \mu^2\hat{\phi}_1^{(2)} + \cdots, \tag{2.29a}$$

$$\hat{\phi}_2 = \hat{\phi}_2^{(0)} + \mu\hat{\phi}_2^{(1)} + \mu^2\hat{\phi}_2^{(2)} + \cdots, \tag{2.29b}$$

$$\hat{\eta} = \hat{\eta}^{(0)} + \mu\hat{\eta}^{(1)} + \mu^2\hat{\eta}^{(2)} + \cdots, \tag{2.29c}$$

and also for the instability growth rate λ by

$$\lambda = \mu\lambda^{(1)} + \mu^2\lambda^{(2)} + \cdots. \tag{2.30}$$

Substituting these perturbation expansions (2.29) and (2.30) in the linearized system of equations (2.16), (2.18), and (2.20)–(2.23), we obtain the leading-order equations for $\hat{\phi}_1^{(0)}$, $\hat{\phi}_2^{(0)}$, and $\hat{\eta}^{(0)}$ as follows:

$$\bar{\nabla}^2\hat{\phi}_1^{(0)} = 0 \quad \text{for} \ -H < z < \bar{\eta}, \tag{2.31}$$

$$\bar{\nabla}^2\hat{\phi}_2^{(0)} = 0 \quad \text{for} \ \bar{\eta} < z < +\infty, \tag{2.32}$$

with the boundary condition

$$\hat{\phi}_{1,z}^{(0)} = 0 \quad \text{at} \ z = -H, \tag{2.33}$$

and the far field conditions

$$\hat{\phi}_{2,z}^{(0)} \to 0 \quad \text{as} \ z \to +\infty, \tag{2.34}$$

$$\hat{\phi}_{1,\xi}^{(0)} \to 0 \quad \text{as} \ \xi \to \pm\infty, \tag{2.35}$$

$$\hat{\phi}_{2,\xi}^{(0)} \to 0 \quad \text{as} \ \xi \to \pm\infty. \tag{2.36}$$

The kinematic and dynamic conditions at the interface $z = \bar{\eta}(\xi)$ are given by

$$\mathcal{L}_1\left(\hat{\phi}_1^{(0)}, \hat{\phi}_2^{(0)}, \hat{\eta}^{(0)}\right) = 0, \quad \mathcal{L}_2\left(\hat{\phi}_1^{(0)}, \hat{\phi}_2^{(0)}, \hat{\eta}^{(0)}\right) = 0, \quad \mathcal{L}_3\left(\hat{\phi}_1^{(0)}, \hat{\phi}_2^{(0)}, \hat{\eta}^{(0)}\right) = 0. \tag{2.37a,b,c}$$

Now, the leading-order perturbation solutions are obtained by

$$\hat{\phi}_1^{(0)} = \bar{\phi}_{1,\xi}, \ \hat{\phi}_2^{(0)} = \bar{\phi}_{2,\xi}, \ \hat{\eta}^{(0)} = \bar{\eta}_\xi \tag{2.38}$$

(up to a common constant multiple) by differentiating the original system of equations for the solitary-wave solutions with respect to ξ along the interface $z = \bar{\eta}(\xi)$.

For the next order $O(\mu)$, we have

$$\bar{\nabla}^2\hat{\phi}_1^{(1)} = 0 \quad \text{for} \ -H < z < \bar{\eta}, \tag{2.39a}$$

$$\bar{\nabla}^2\hat{\phi}_2^{(1)} = 0 \quad \text{for} \ \bar{\eta} < z < +\infty, \tag{2.39b}$$

with

$$\hat{\phi}_{1,z}^{(1)} = 0 \quad \text{at} \ z = -H, \tag{2.40a}$$

$$\hat{\phi}_{2,z}^{(1)} \to 0 \quad \text{as} \ z \to +\infty, \tag{2.40b}$$

$$\hat{\phi}_{1,\xi}^{(1)} \to 0 \quad \text{as} \ \xi \to \pm\infty, \tag{2.40c}$$

$$\hat{\phi}_{2,\xi}^{(1)} \to 0 \quad \text{as} \ \xi \to \pm\infty, \tag{2.40d}$$

and with the kinematic and dynamic conditions at the interface $z = \bar{\eta}(\xi)$ given by

$$\mathcal{L}_1\left(\hat{\phi}_1^{(1)}, \hat{\phi}_2^{(1)}, \hat{\eta}^{(1)}\right) = -\lambda^{(1)}\hat{\eta}^{(0)} = -\lambda^{(1)}\bar{\eta}_\xi, \tag{2.41a}$$

$$\mathcal{L}_2\left(\hat{\phi}_1^{(1)}, \hat{\phi}_2^{(1)}, \hat{\eta}^{(1)}\right) = -\lambda^{(1)}\hat{\eta}^{(0)} = -\lambda^{(1)}\bar{\eta}_\xi, \tag{2.41b}$$

$$\mathcal{L}_3\left(\hat{\phi}_1^{(1)}, \hat{\phi}_2^{(1)}, \hat{\eta}^{(1)}\right) = -\lambda^{(1)}\left(\hat{\phi}_1^{(0)} - R\hat{\phi}_2^{(0)}\right) = -\lambda^{(1)}\left(\bar{\phi}_{1,\xi} - R\bar{\phi}_{2,\xi}\right). \tag{2.41c}$$

And then, the second-order perturbations are solved to give

$$\hat{\phi}_1^{(1)} = -\lambda^{(1)}\bar{\phi}_{1,V}, \quad \hat{\phi}_2^{(1)} = -\lambda^{(1)}\bar{\phi}_{2,V}, \quad \hat{\eta}^{(1)} = -\lambda^{(1)}\bar{\eta}_V \tag{2.42}$$

by differentiating with respect to the solitary wavespeed V to the original system of equations for the plane solitary-wave solutions.

For the next-order perturbations of $O(\mu^2)$, we have

$$\bar{\nabla}^2\hat{\phi}_1^{(2)} = \hat{\phi}_1^{(0)} = \bar{\phi}_{1,\xi} \quad \text{for } -H < z < \bar{\eta}, \tag{2.43a}$$

$$\bar{\nabla}^2\hat{\phi}_2^{(2)} = \hat{\phi}_2^{(0)} = \bar{\phi}_{2,\xi} \quad \text{for } \bar{\eta} < z < +\infty, \tag{2.43b}$$

with

$$\hat{\phi}_{1,z}^{(2)} = 0 \quad \text{at } z = -H, \tag{2.44a}$$

$$\hat{\phi}_{1,\xi}^{(2)} \to 0 \quad \text{as } \xi \to \pm\infty, \tag{2.44b}$$

$$\hat{\phi}_{2,\xi}^{(2)} \to 0 \quad \text{as } \xi \to \pm\infty, \tag{2.44c}$$

$$\hat{\phi}_{2,z}^{(2)} \to 0 \quad \text{as } z \to +\infty, \tag{2.44d}$$

with the kinematic and dynamic conditions at the interface $z = \bar{\eta}(\xi)$ given by

$$\mathcal{L}_1\left(\hat{\phi}_1^{(2)}, \hat{\phi}_2^{(2)}, \hat{\eta}^{(2)}\right) = -\lambda^{(1)}\hat{\eta}^{(1)} - \lambda^{(2)}\hat{\eta}^{(0)} = \lambda^{(1)2}\bar{\eta}_V - \lambda^{(2)}\bar{\eta}_\xi, \tag{2.45a}$$

$$\mathcal{L}_2\left(\hat{\phi}_1^{(2)}, \hat{\phi}_2^{(2)}, \hat{\eta}^{(2)}\right) = -\lambda^{(1)}\hat{\eta}^{(1)} - \lambda^{(2)}\hat{\eta}^{(0)} = \lambda^{(1)2}\bar{\eta}_V - \lambda^{(2)}\bar{\eta}_\xi, \tag{2.45b}$$

$$\mathcal{L}_3\left(\hat{\phi}_1^{(2)}, \hat{\phi}_2^{(2)}, \hat{\eta}^{(2)}\right) = -\lambda^{(1)}\left(\hat{\phi}_1^{(1)} - R\hat{\phi}_2^{(1)}\right) - \lambda^{(2)}\left(\hat{\phi}_1^{(0)} - R\hat{\phi}_2^{(0)}\right) - \frac{\hat{\eta}^{(0)}}{\sqrt{1 + \bar{\eta}_\xi^2}}$$

$$= \lambda^{(1)2}\left(\bar{\phi}_{1,V} - R\bar{\phi}_{2,V}\right) - \lambda^{(2)}\left(\bar{\phi}_{1,\xi} - R\bar{\phi}_{2,\xi}\right) - \frac{\bar{\eta}_\xi}{\sqrt{1 + \bar{\eta}_\xi^2}}. \tag{2.45c}$$

2.5 Solvability condition for the perturbations of $O(\mu^2)$

In order to have solutions that do not blow up for the perturbations $\hat{\phi}_1^{(2)}$, $\hat{\phi}_2^{(2)}$, and $\hat{\eta}^{(2)}$ from (2.43)–(2.45) as $\xi \to \pm\infty$, it is required that they solve the following adjoint boundary-value problem:

$$\bar{\nabla}^2\psi_1 = 0 \quad \text{for } -H < z < \bar{\eta}, \tag{2.46a}$$

$$\bar{\nabla}^2\psi_2 = 0 \quad \text{for } \bar{\eta} < z < +\infty, \tag{2.46b}$$

with the boundary condition

$$\psi_{1,z} = 0 \quad \text{at } z = -H, \tag{2.47}$$

with the far-field conditions

$$\psi_{2,z} \to 0 \quad \text{as } z \to +\infty, \tag{2.48a}$$

$$\psi_{1,\xi} \to 0 \quad \text{as } \xi \to \pm\infty, \tag{2.48b}$$

$$\psi_{2,\xi} \to 0 \quad \text{as } \xi \to \pm\infty, \tag{2.48c}$$

and with the kinematic and dynamic conditions at the interface $z = \bar{\eta}(\xi)$

$$\mathcal{L}_1^+ (\psi_1, \psi_2, \zeta) = 0, \tag{2.49a}$$

$$\mathcal{L}_2^+ (\psi_1, \psi_2, \zeta) = 0, \tag{2.49b}$$

$$\mathcal{L}_3^+ (\psi_1, \psi_2, \zeta) = 0, \tag{2.49c}$$

where

$$\mathcal{L}_1^+ \equiv -\sqrt{1 + \bar{\eta}_\xi^2} \frac{\partial}{\partial \vec{n}_1} \psi_1 - \left\{ \frac{\mathrm{d}}{\mathrm{d}\xi} \bar{\phi}_{1,\xi} + \left(-V + \bar{\phi}_{1,\xi} \right) \frac{\mathrm{d}}{\mathrm{d}\xi} \right\} \zeta, \tag{2.50a}$$

$$\mathcal{L}_2^+ \equiv \sqrt{1 + \bar{\eta}_\xi^2} \frac{\partial}{\partial \vec{n}_2} \psi_2 + R \left\{ \frac{\mathrm{d}}{\mathrm{d}\xi} \bar{\phi}_{2,\xi} + \left(-V + \bar{\phi}_{2,\xi} \right) \frac{\mathrm{d}}{\mathrm{d}\xi} \right\} \zeta, \tag{2.50b}$$

$$\mathcal{L}_3^+ \equiv - \left(-V + \bar{\phi}_{1,\xi} \right) \frac{\mathrm{d}}{\mathrm{d}\xi} \psi_1 - \left(-V + \bar{\phi}_{2,\xi} \right) \frac{\mathrm{d}}{\mathrm{d}\xi} \psi_2$$

$$+ \sqrt{1 + \bar{\eta}_\xi^2} \left\{ \left(-V + \bar{\phi}_{1,\xi} \right) \frac{\partial}{\partial \vec{n}_1} \bar{\phi}_{1,\xi} + R \left(-V + \bar{\phi}_{2,\xi} \right) \frac{\partial}{\partial \vec{n}_2} \bar{\phi}_{2,\xi} \right\} \zeta + (1 - R) \zeta - \left\{ \frac{\zeta_\xi}{\left(1 + \bar{\eta}_\xi^2 \right)^{\frac{3}{2}}} \right\}_\xi . \tag{2.50c}$$

The above adjoint boundary-value problem is solved by

$$\psi_1 = \bar{\phi}_{1,\xi}, \quad \psi_2 = -R\bar{\phi}_{2,\xi}, \quad \zeta = -\bar{\eta}_\xi \tag{2.51}$$

(up to any constant multiple of the above).

Applying integration by parts along the fluid interface $z = \eta(\xi)$ and Green's second identity on both upper and lower fluid layers (the orientations of the boundary integrals are opposite in the upper and lower layers), the leading-order terms appear in $O(\mu^2)$ from (2.29), (2.30), (2.37a,b,c), (2.38), (2.41), (2.42), (2.45), (2.50), and (2.51), such that

$$0 = \int_{-\infty}^{+\infty} \lambda^{(1)2} \left\{ \left(\bar{\phi}_{1,\xi} - R\bar{\phi}_{2,\xi} \right) \bar{\eta}_V - \left(\bar{\phi}_{1,V} - R\bar{\phi}_{2,V} \right) \bar{\eta}_\xi \right\} \Big|_{z=\bar{\eta}} \mathrm{d}\xi$$

$$+ \int_{-\infty}^{+\infty} \left\{ \left(\int_{-H}^{\bar{\eta}} \bar{\phi}_{1,\xi}^2 \mathrm{d}z + R \int_{\bar{\eta}}^{+\infty} \bar{\phi}_{2,\xi}^2 \mathrm{d}z \right) + \frac{\bar{\eta}_\xi^2}{\sqrt{1 + \bar{\eta}_\xi^2}} \right\} \mathrm{d}\xi. \tag{2.52}$$

2.6 Instability criterion in terms of the total mechanical energy of solitary-wave solutions

As in [15], the total mechanical energy of a solitary wave $\mathcal{E}$ is defined by

$$\mathcal{E} = \mathcal{K} + \mathcal{G} + \mathcal{T}, \tag{2.53}$$

where

$$\mathcal{K} = \frac{1}{2} \int_{-\infty}^{+\infty} \left(\int_{-H}^{\bar{\eta}} \left| \bar{\nabla} \bar{\phi}_1 \right|^2 \mathrm{d}z + R \int_{\bar{\eta}}^{+\infty} \left| \bar{\nabla} \bar{\phi}_2 \right|^2 \mathrm{d}z \right) \mathrm{d}\xi = -\frac{1}{2} V \int_{-\infty}^{+\infty} \left\{ \left(\bar{\phi}_1 - R\bar{\phi}_2 \right) \bar{\eta}_\xi \right\} \Big|_{z=\bar{\eta}} \mathrm{d}\xi \tag{2.54}$$

denotes the kinetic energy for $\bar{\nabla} = (\partial/\partial\xi, \partial/\partial z)$,

$$\mathcal{G} = \frac{1 - R}{2} \int_{-\infty}^{+\infty} \bar{\eta}^2 \, \mathrm{d}\xi \tag{2.55}$$

the gravitational potential energy, and

$$\mathcal{T} = \int\limits_{-\infty}^{+\infty} \left(\sqrt{1 + \bar{\eta}_\xi^2} - 1 \right) \, \mathrm{d}\xi \tag{2.56}$$

the potential energy due to the interfacial tension. This definition for the total mechanical energy of interfacial gravity–capillary solitary waves was also adopted in [29,30], except for the way of nondimensionalization.

Then, it is shown that

$$\frac{\partial \mathcal{E}}{\partial V} = V \int\limits_{-\infty}^{+\infty} \left\{ \left(\bar{\phi}_{1,\xi} - R\bar{\phi}_{2,\xi} \right) \bar{\eta}_V - \left(\bar{\phi}_{1,V} - R\bar{\phi}_{2,V} \right) \bar{\eta}_\xi \right\}\big|_{z=\bar{\eta}} \, \mathrm{d}\xi \tag{2.57}$$

by using integration by parts along the fluid interface and Green's first identity on both upper and lower fluid layers. Hence, the leading-order coefficient $\lambda^{(1)}$ for the instability growth rate in μ is expressed by

$$\lambda^{(1)^2} = - \frac{\int_{-\infty}^{+\infty} \left\{ \left(\int_{-H}^{\bar{\eta}} \bar{\phi}_{1,\xi}^2 \mathrm{d}z + R \int_{\bar{\eta}}^{+\infty} \bar{\phi}_{2,\xi}^2 \mathrm{d}z \right) + \frac{\bar{\eta}_\xi^2}{\sqrt{1 + \bar{\eta}_\xi^2}} \right\} \mathrm{d}\xi}{\frac{1}{V} \frac{\partial \mathcal{E}}{\partial V}}. \tag{2.58}$$

Therefore, if the total mechanical energy of the solitary waves is a decreasing function of V, then $\lambda^{(1)^2}$ becomes positive. This implies that a positive instability growth rate can exist for each real value of μ, so that the solitary waves are unstable under any long-wave transverse disturbances. Note that the final expression (2.58) for the leading-order coefficient of the instability growth rate is not affected by any constant multiple factor that may be applied to the perturbed solutions.

3 Estimate of the long-wave transverse instability growth rate for the interfacial gravity–capillary solitary waves in deep water

3.1 Weakly nonlinear solitary wavepacket solutions in the long-wave limit

Under the close-density condition

$$1 - R = O(\epsilon) \quad \text{and} \quad H = O(1), \tag{3.1}$$

the derivation of the weakly nonlinear long-wave Benjamin model equation

$$\frac{1}{V_0} \eta_t + \eta_x + \frac{3}{4H} \left(\eta^2 \right)_x - \frac{RH}{2} \mathcal{H}\{\eta_{xx}\} - \frac{1}{2(1-R)} \eta_{xxx} = 0 \tag{3.2}$$

is provided in the Appendix. It is known that the steady Benjamin equation of a canonical form

$$\eta^* - \eta^{*2} - 2\gamma \mathcal{H}^* \left\{ \eta_{\xi^*}^* \right\} - \eta_{\xi^*\xi^*}^* = 0 \tag{3.3}$$

allows solitary-wave solutions for $0 < \gamma < 1$ (see [10]). Applying a simple scaling

$$\eta(\xi) = \frac{1}{\beta} \eta^*(\xi^*), \quad \xi^* = \alpha\xi \tag{3.4}$$

for

$$\alpha = \frac{(1-R)RH}{2\gamma}, \quad \beta = -\frac{6\gamma^2}{(1-R)R^2H^3}, \tag{3.5}$$

we have that $\eta(\xi) = \eta(x - Vt)$ satisfies (3.2) where

$$\gamma^2 = \frac{(1-R)R^2H^2}{8} \cdot \frac{V_0}{V_0 - V}, \quad V_0 = \sqrt{(1-R)H}. \tag{3.6}$$

$0 < \gamma < 1$ imposes on (3.6) the condition

$$V < \left\{ 1 - \frac{(1-R)\,R^2H^2}{8} \right\} V_0. \tag{3.7}$$

A remarkable concurrence is found that the right-hand side of (3.7) is the minimum phase speed from the long-wave dispersion relation (2.11), which is attained for a pair of nonzero critical wavenumbers

$$k_0 = \pm \frac{(1-R)\,RH}{2}. \tag{3.8}$$

The amplitudes of the solitary-wave solutions of (3.2) become arbitrarily small if the two densities are close enough in their values or if the nondimensional depth is sufficiently shallow.

From (3.3), a weakly nonlinear solitary long-wavepacket bifurcates in the form of

$$\eta^*(\xi^*) = \pm \frac{2}{\sqrt{3}}\epsilon\,\mathrm{sech}\left(\epsilon\xi^*\right)\cos\xi^* + \frac{4}{3}\epsilon^2\mathrm{sech}^2\left(\epsilon\xi^*\right)\cos^2\xi^* + O(\epsilon^3) \tag{3.9}$$

for $\gamma = 1 - \epsilon^2/2$ (see [14]). The corresponding solitary wavepacket for (3.9) is given by

$$\eta\left(\xi\right) \sim \mp \frac{(1-R)\,R^2H^3}{3\sqrt{3}}\epsilon\,\mathrm{sech}\left(\epsilon k_0\xi\right)\cos\left(k_0\xi\right)\cdots. \tag{3.10}$$

The sign of the leading-order expression for the solitary wavepacket is reversed when (3.3) is transformed into (3.2) via (3.4)–(3.6), so that the elevation solitary wavepacket (3.9) becomes the depression one (3.10), which should be stable under longitudinal disturbances according to [12].

From (B.2) and (B.3), the two potential functions are estimated as follows:

$$\bar{\phi}_{1,\xi}(\xi,z) = \sqrt{\frac{1-R}{H}}\bar{\eta}(\xi) + O(\epsilon^2) \sim \mp \frac{(1-R)^{\frac{3}{2}}\,R^2H^{\frac{5}{2}}}{3\sqrt{3}}\epsilon\,\mathrm{sech}\left(\epsilon k_0\xi\right)\cos\left(k_0\xi\right) \tag{3.11}$$

for $-H < z < \bar{\eta}(\xi)$, and

$$\bar{\phi}_{2,\xi}(\xi,z) = -V_0\mathcal{F}^{-1}\left\{ |k|\,\mathrm{e}^{-kz}\mathcal{F}\left\{\eta(\xi)\right\}(k) \right\} + O(\epsilon^2)$$
$$\sim \pm \frac{(1-R)^{\frac{5}{2}}\,R^3H^{\frac{9}{2}}}{6\sqrt{3}}\epsilon\,\mathrm{sech}\left(\epsilon k_0\xi\right)\cos\left(k_0\xi\right)\mathrm{e}^{-k_0z} \tag{3.12}$$

for $\bar{\eta}(\xi) < z < +\infty$.

Substituting (3.10), (3.11), and (3.12) in (2.53)–(2.56), we obtain

$$\mathcal{K} \sim \frac{\epsilon}{27}\left(1-R\right)^2R^3H^5\left\{ 1 + \frac{(1-R)\,R^2H^2}{2} \right\}, \tag{3.13a}$$

$$\mathcal{G} \sim \frac{\epsilon}{27}\left(1-R\right)^2R^3H^5, \tag{3.13b}$$

$$\mathcal{T} \sim \frac{\epsilon}{108}\left(1-R\right)^3R^5H^7, \tag{3.13c}$$

$$\mathcal{E} \sim \frac{\epsilon}{27}\left(1-R\right)^2R^3H^5\left\{ 2 + \frac{3\left(1-R\right)\,R^2H^2}{4} \right\}. \tag{3.13d}$$

Accordingly, (2.57) becomes

$$\frac{\mathcal{E}_V}{V} \sim -\frac{8}{27}\epsilon^{-1}RH^2\frac{8 + 3\left(1-R\right)\,R^2H^2}{8 - \left(1-R\right)\,R^2H^2} < 0 \tag{3.14}$$

for fixed R and H. Hence, the associated positive eigenvalue is estimated from (2.58) by

$$\lambda^{(1)} \sim \epsilon\sqrt{2\left(V_{\min} - V\right)V_0}. \tag{3.15}$$

The instability growth rate in terms of the order of $|V_{\min} - V|$ is consistent with the result for the surface gravity–capillary solitary waves in [15].

We now conclude that an instability occurs for the weakly nonlinear solitary long-wavepackets for arbitrarily small $\epsilon > 0$ under long-wave disturbances in the transverse direction to the wave propagation.

In comparison with the instability growth rate that was computed from the Benjamin model equation, Sect. 4 in [14] is reviewed ($\eta\,(\xi)$ in there corresponds to $\eta^*\,(\xi^*)$ in this section). In terms of $\eta^*\,(\xi^*)$, the instability growth rate in the leading order is expressed by

$$\sqrt{\frac{4\int_{-\infty}^{+\infty}\eta^{*2}\mathrm{d}\xi^*}{3\int_{-\infty}^{+\infty}\eta^{*2}\mathrm{d}\xi^* - \gamma\frac{\partial}{\partial\gamma}\int_{-\infty}^{+\infty}\eta^{*2}\mathrm{d}\xi^*}} \sim 2\epsilon \tag{3.16}$$

for the same $\gamma = 1 - \epsilon^2/2$ as that used in this section. The scaling

$$\hat{T} = \frac{\alpha^3 V_0}{2\,(1-R)}t, \quad \xi^* = \alpha\xi, \quad \hat{Z} = \frac{\alpha^2}{\sqrt{1-R}}y \tag{3.17}$$

is needed for Eq. 4.2 in [14] in order to obtain the associated two-dimensional weakly nonlinear long-wave model equation (A.28) for the nondimensionalization used here. By multiplying (3.16) by

$$\frac{\alpha^3 V_0}{2\,(1-R)}\cdot\frac{\sqrt{1-R}}{\alpha^2} = \frac{\alpha V_0}{2\sqrt{1-R}}, \tag{3.18}$$

we observe that the leading-order instability growth rate derived from the Benjamin model equation matches (3.15).

3.2 Fully nonlinear interfacial gravity–capillary solitary waves

With or without the constraint of the long-waveness assumption, it is expected to obtain fully nonlinear interfacial gravity–capillary plane solitary waves by varying $0 < R < 1$ and $V < V_{\min}$ continuously from the weakly nonlinear solitary wavepacket solutions. In this study, it is highlighted that the total mechanical energy of the solitary waves decreases with respect to the solitary wavespeed near the bifurcation points. Solitary-wave solutions are expected to be highly nonlinear as they are farther below from the bifurcation points in the bifurcation diagram. Hence, the long-wave transverse instability should occur as well for the associated fully nonlinear solitary waves within certain ranges when the solitary wavespeed is close to the minimum wavespeed and when the density ratio is close to the unity.

4 Discusssion

The reason why long-wave disturbances are examined for the effect of transverse instability can be explained as follows. For transversely unperturbed plane solitary waves, only the zeroth wave mode in the transverse direction is available. Although the instability bandwidth in the transverse direction is not precisely computed, it is certain that nearby modes, which are among long-wave or side-band modes, to the zeroth mode in the transverse direction should be excited or stabilized at the initial stage when disturbances are applied. Therefore, it is justified that most efforts are made in this study to verify (1.1) as well as to obtain the analytical explicit expression of the leading-order instability growth rate for long-wave transverse perturbations in terms of the interfacial gravity–capillary solitary-wave solutions.

The criterion (1.1) is applicable only for solitary waves that can be parameterized by the wavespeed, not for isolated solitary waves that feature discrete wavespeeds. The existence of isolated solitary waves can be explained in terms of a homoclinic orbit that passes through the origin when the equations for steady solitary-wave solutions are expressed in an equivalent spatial dynamical system. For instance, isolated interfacial solitary waves were computed under the rotational-flow assumption in [31]. See [32] for general statements for the bifurcation of such isolated solitary waves. In this study, however, any stability issues regarding to isolated solitary waves are not addressed.

The analysis provided here has nothing to do with the shape of solitary wavepackets, elevation or depression. It is straightforward to extend the same analysis for a potential flow of two finite depth layers as in [9]. It will be interesting to see whether the result in this study, where the finite-depth layer is at the bottom of the fluid system, qualitatively agrees with those of the gravity–capillary surface solitary waves discussed in [3,6–8,16] in the limit of $R \to 0$ in view of the dispersion relation, the type of the longitudinally stable solitary waves (elevation or depression), the long-wave transverse instability, and the order of the instability growth rate in terms of the wavespeed difference from the critical value.

Often, it is known that two branches of solitary waves emanate from the bifurcation point. See [9,10,12,14] for the result on the computation of two branches of interfacial gravity–capillary solitary waves. The counterparts for surface gravity–capillary solitary waves are described in [7,8,11]. In those works, one branch is stable and the other is unstable under longitudinal disturbances. For the physical setting where the finite-depth fluid layer is on top of the fluid system, it is verified in [12] in the framework of the full Euler equations that the elevation interfacial gravity–capillary solitary waves, of which the center peak is concave, are the stable ones, whereas the depressed ones with the convex center peak are unstable under small longitudinal perturbations. Even when the finite-depth fluid layer is located at the bottom of the fluid system, the stability result should be identical, except that the actual shape of the solitary waves in the latter configuration are upside-down with respect to the former ones (see Appendix for a detailed analysis).

Actually, the criteria for the longitudinal and transverse stability of solitary waves seem to be related. In principle, the exchange of the longitudinal stability of solitary waves should occur whenever the continuously parameterized solutions to the nonlinear system that governs the solitary waves pass through a turning point in the bifurcation diagram. For gravity solitary waves, in particular, it was confirmed that the criterion (1.1) itself determines the longitudinal stability by showing that the exchange of longitudinal stability occurs at every stationary point of the total mechanical energy of gravity solitary waves (see [33,34] for the result on surface gravity solitary waves, and [18] for interfacial gravity solitary waves). Note that (1.1) plays a role as a sufficient condition for the transverse instability of the interfacial gravity–capillary solitary waves as in [13,15,17]. Indeed, we may expect to enhance the analytical result for the long-wave transverse instability criterion for the interfacial gravity–capillary solitary waves by performing a detailed higher-order analysis near the far field of the solitary waves as the associated results for the surface gravity solitary waves in [13,18].

It is useful to define the impulse and circulation of interfacial gravity–capillary solitary waves in a fashion similar to the counterparts of surface water waves [35] because those quantities are closely related with the transverse instability criterion. The impulse of the interfacial gravity–capillary solitary waves in deep water is defined by

$$
\begin{aligned}
\mathcal{I} &= \int_{-\infty}^{+\infty} \mathrm{d}\xi \left(\int_{-H}^{\bar{\eta}} \bar{\phi}_{1,\xi} \,\mathrm{d}z + R \int_{\bar{\eta}}^{+\infty} \bar{\phi}_{2,\xi} \,\mathrm{d}z \right) \\
&= \left(\int_{-H}^{\bar{\eta}} \bar{\phi}_1 \,\mathrm{d}z + R \int_{\bar{\eta}}^{+\infty} \bar{\phi}_2 \,\mathrm{d}z \right)\Bigg|_{\xi=-\infty}^{+\infty} - \int_{-\infty}^{+\infty} \left\{ \left(\bar{\phi}_1 - R\bar{\phi}_2 \right) \bar{\eta}_\xi \right\}\big|_{z=\bar{\eta}} \,\mathrm{d}\xi \\
&= H\mathcal{C} + G.
\end{aligned}
\tag{4.1}
$$

In the above expression,

$$
\mathcal{C} = \bar{\phi}_1\big|_{\xi=-\infty}^{+\infty}
\tag{4.2}
$$

is the circulation of the lower-layer potential function in the finite-depth layer. The quantity

$$
R \int_{\bar{\eta}}^{+\infty} \bar{\phi}_2\big|_{\xi=-\infty}^{+\infty} \,\mathrm{d}z
\tag{4.3}
$$

vanishes because so does $\bar{\phi}_2$ as either z or $|\xi|$ goes to infinity. As a matter of fact,

$$G = - \int\limits_{-\infty}^{+\infty} \left\{ (\bar{\phi}_1 - R\bar{\phi}_2) \, \bar{\eta}_\xi \right\}\big|_{z=\bar{\eta}} \, \mathrm{d}\xi \tag{4.4}$$

satisfies

$$\frac{\partial G}{\partial V} = \frac{1}{V} \frac{\partial \mathcal{E}}{\partial V}, \tag{4.5}$$

which can be shown by using integration by parts. As indicated in [15], (1.1) is sufficient for the long-wave transverse instability of solitary waves whether the circulation of solitary waves is nontrivial or not. For circulation-free solitary waves, the impulse change rate of solitary waves with respect to the wavespeed, which was used for a transverse instability criterion for the solitary water waves in [33] and used for the longitudinal stability criterion for the solitary water waves in [34], is equal to $\partial \mathcal{E}/\partial V$. In general, the circulation of solitary waves does not necessarily vanish when a fluid layer is bounded by a wall because the fluid is allowed to slip on the boundary in the potential-flow assumption.

For a future study, rigorous mathematical proofs for the transverse instability of gravity–capillary solitary waves and the existence of gravity–capillary lumps, either for interfacial and surface wave problem, especially in the weak interfacial or surface-tension regime, can be made; there are recent related studies in the strong surface-tension regime [36,37] although the type of gravity–capillary solitary waves they have studied are different from what is discussed in this study.

Appendix

This appendix presents, under the close-density condition, a derivation of the weakly nonlinear long-wave model equation for interfacial gravity–capillary waves in two-layer potential flows in deep water.

A. Two-dimensional Benjamin model equation (2-DB)

Under the close-density condition (1.3), the weakly nonlinear model equation for the interfacial gravity–capillary waves in a two-layer potential flow in deep water has been derived in [16]. Here, an equivalent derivation is presented, assuming that the finite-depth layer is on the bottom of the fluid system. Thus, the derivation is based on (2.1), (2.2a), (2.7)–(2.9), and (2.11), as discussed in Sect. 2.

Let us assume that (3.1) is satisfied and that the characteristic wave length is measured by $\epsilon \sim \kappa$. Assuming that the y-directional component of interfacial waves varies more slowly than the x-directional one, say $l \sim \sqrt{\epsilon}k$, we may approximate both (2.9) and (2.11) by

$$\omega = \pm\sqrt{(1-R)\, Hk} \left\{ 1 - \frac{1}{2}RH|k| + \frac{1}{2(1-R)}k^2 + \frac{l^2}{2k^2} + O(\epsilon^2) \right\}. \tag{A.1}$$

If we consider the uni-directional part of the waves, only the positive part from (A.1) can be taken for $k > 0$. Then, the linear terms of the long-wave model equation are completely recovered by the relations

$$\omega \to \mathrm{i}\frac{\partial}{\partial t}, \quad k \to -\mathrm{i}\frac{\partial}{\partial x}, \quad l \to -\mathrm{i}\frac{\partial}{\partial y}, \quad |k| \to \frac{\partial}{\partial x}\mathcal{H}\{\cdot\}, \tag{A.2}$$

where $\mathcal{H}\{\cdot\}$ is the Hilbert transformation defined by

$$\mathcal{H}\left\{f(x')\right\}(x) = \frac{1}{\pi} \int\limits_{-\infty}^{+\infty} \frac{f(x')}{x - x'}\mathrm{d}x'. \tag{A.3}$$

In [12,14], the Hilbert transformation is defined as the negative sign of (A.3), but (A.3) seems to be natural as the convolution of $f(x)$ with $1/(\pi x)$. The Fourier transformation of $1/x$ is given by

$$\mathcal{F}\left\{\frac{1}{x}\right\}(k) = \frac{1}{2\pi}\int\limits_{-\infty}^{+\infty}\frac{e^{-ikx}}{x}dx = -i\frac{\text{sign}(k)}{2} \tag{A.4}$$

in the sense of a principal-value integral.

From the long-wave approximation, the speed of the fast moving wave component is $V_0 = \sqrt{(1-R)H} \sim \sqrt{\epsilon}$ and the rest of the wave components is at most $O(\epsilon^{\frac{3}{2}})$. Regarding that the interfacial elevation is much smaller than the nondimensional finite depth H of the lower fluid layer and that the upper layer potential function varies in the vertical direction to a comparable degree to the x-directional variance but is weaker than the lower-layer potential of the finite depth, the following scaling is naturally chosen:

$$\xi' = \epsilon(x - V_0 t), \quad y' = \epsilon^{\frac{3}{2}}y, \quad z' = z \text{ (lower)}, \quad Z' = \epsilon z \text{ (upper)}, \tag{A.5a}$$

$$t' = \epsilon^2 V_0 t, \quad \eta' = \epsilon^{-1}\eta, \quad \phi'_1 = V_0^{-1}\phi_1, \quad \phi'_2 = (\epsilon V_0)^{-1}\phi_2. \tag{A.5b}$$

By doing so, we make the nondimensional physical quantities, expressed by the new variables with the prime symbol, to be $O(1)$ when they are observed in the frame moving with the speed V_0 in the positive x-direction.

In terms of the new variables, the Euler equations are written by

$$\epsilon^2\phi_{1,\xi'\xi'} + \epsilon^3\phi_{1,y'y'} + \phi_{1,z'z'} = 0, \quad -H < z' < \epsilon\eta'(\xi', y', t'), \tag{A.6a}$$

$$\phi_{2,\xi'\xi'} + \phi_{2,Z'Z'} = O(\epsilon), \quad \epsilon^2\eta'(\xi', y', t') < Z' < +\infty, \tag{A.6b}$$

and on the interface $Z' = \epsilon z' = \epsilon^2\eta'(\xi', y', t')$:

$$\epsilon^2\left(-\eta'_{\xi'} + \epsilon\eta'_{t'} + \epsilon\phi'_{1,\xi'}\eta'_{\xi'}\right) - \phi'_{1,z'} = O(\epsilon^4), \tag{A.7a}$$

$$-\eta'_{\xi'} + \epsilon\eta'_{t'} + \phi'_{2,\xi'}\eta'_{\xi'} - \epsilon^2\phi'_{2,Z'} = O(\epsilon^3), \tag{A.7b}$$

$$\epsilon V_0^2\left\{-\left(\phi'_{1,\xi'} - \epsilon R\phi'_{2,\xi'}\right) + \epsilon\left(\phi'_{1,t'} - \epsilon R\phi'_{2,t'}\right)\right\}$$

$$+ \frac{1}{2}V_0^2\left\{\left(\epsilon^2\phi'^2_{1,\xi'} + \epsilon^3\phi'^2_{1,y'} + \phi'^2_{1,z}\right) - \epsilon^4 R\left(\phi'^2_{2,\xi'} + \epsilon\phi'^2_{2,y'} + \phi'^2_{2,Z'}\right)\right\}$$

$$+ \epsilon(1-R)\eta' - \epsilon^3\eta'_{\xi'\xi'} = O(\epsilon^4), \tag{A.7c}$$

with

$$\phi'_{1,z'} = 0 \quad \text{at } z' = -H, \tag{A.8a}$$

$$\phi'_{1,\xi'} \to 0 \quad \text{as } \xi' \to \pm\infty, \tag{A.8b}$$

$$\phi'_{1,y'} \to 0 \quad \text{as } y' \to \pm\infty, \tag{A.8c}$$

$$\phi'_{2,Z'} \to 0 \quad \text{as } Z' \to +\infty, \tag{A.8d}$$

$$\phi'_{2,\xi'} \to 0 \quad \text{as } \xi' \to \pm\infty, \tag{A.8e}$$

$$\phi'_{2,y'} \to 0 \quad \text{as } y' \to \pm\infty. \tag{A.8f}$$

The right-hand sides in (A.6) and (A.7) involve the terms with the y-derivatives and the next order remainders from the interfacial tension terms.

Expanding ϕ'_1 in ϵ by

$$\phi'_1 = \phi'^{(0)}_1 + \epsilon\phi'^{(1)}_1 + \epsilon^2\phi'^{(2)}_1 + \epsilon^3\phi'^{(3)}_1 + \cdots, \tag{A.9}$$

(A.6a) is solved in successive order up to $O(\epsilon^2)$ with the bottom boundary condition (A.8a) to obtain

$$\phi'_1 = \theta'^{(0)} + \epsilon\theta'^{(1)} + \epsilon^2\left\{\theta'^{(2)} - \frac{1}{2}(z'+H)^2\theta'^{(0)}_{\xi'\xi'}\right\}$$

$$+ \epsilon^3\left\{\theta'^{(3)} - \frac{1}{2}(z'+H)^2\left(\theta'^{(1)}_{\xi'\xi'} + \theta'^{(0)}_{y'y'}\right)\right\} + O(\epsilon^4), \tag{A.10}$$

where $\theta'^{(0)}, \theta'^{(1)}, \theta'^{(2)}, \theta'^{(3)}, \ldots$ are independent of z, because

$$\phi'^{(0)}_{1,z'z'} = 0, \quad \phi'^{(1)}_{1,z'z'} = 0, \quad \phi'^{(2)}_{1,z'z'} = -\phi'^{(0)}_{1,\xi'\xi'} = -\theta'^{(0)}_{\xi'\xi'}, \tag{A.11a}$$

$$\phi'^{(3)}_{1,z'z'} = -\phi'^{(1)}_{1,\xi'\xi'} - \phi'^{(0)}_{1,y'y'} = -\theta'^{(1)}_{\xi'\xi'} - \theta'^{(0)}_{y'y'} \tag{A.11b}$$

in $-H < z' < \epsilon\eta'$, with

$$\phi'^{(0)}_{1,z'} = \phi'^{(1)}_{1,z'} = \phi'^{(2)}_{1,z'} = \phi'^{(3)}_{1,z'} = 0 \quad \text{on} \quad z' = -H. \tag{A.12}$$

The upper-layer potential ϕ_2 is approximated in terms of the inverse Fourier transformation with respect to ξ'

$$\phi'_2\left(\xi', y', Z', t'\right) = \int_{-\infty}^{+\infty} \mathcal{F}'\left\{\phi'_2\left(\xi', y', Z', t'\right)\right\}(k')e^{ik'\xi' - |k'|Z'}dk' + O(\epsilon), \tag{A.13}$$

where

$$\mathcal{F}'\left\{f(\xi')\right\}(k') = \frac{1}{2\pi}\int_{-\infty}^{+\infty} f(\xi')e^{-ik'\xi'}d\xi' \tag{A.14}$$

for

$$k = \epsilon k'. \tag{A.15}$$

Now, the Fourier transformation of (A.7b) with respect to ξ' is taken for $Z' = \epsilon^2\eta'(\xi', y', t') \ll 1$ to yield

$$\mathcal{F}'\left\{\phi'_{2,Z'}\big|_{Z'=\epsilon^2\eta'(\xi',y',t')}\right\}(k') = -\left|k'\right|\mathcal{F}'\left\{\phi'_2\big|_{Z'=\epsilon^2\eta'(\xi',y',t')}\right\}(k')$$
$$= -ik'\mathcal{F}'\left\{\eta'\right\}(k') + O(\epsilon), \tag{A.16}$$

and thus,

$$\mathcal{F}'\left\{\phi'_2\big|_{Z'=\epsilon^2\eta'(\xi',y',t')}\right\}(k') = i\,\text{sign}(k')\mathcal{F}'\left\{\eta'\right\}(k') + O(\epsilon). \tag{A.17}$$

It follows that

$$\phi'_2\big|_{Z'=\epsilon^2\eta'(\xi',y',t')} = -\int_{-\infty}^{+\infty}\frac{\eta'(s, y', t')}{\xi' - s}ds + O(\epsilon)$$
$$= -\mathcal{H}'\left\{\eta'\left(\xi', y', t'\right)\right\} + O(\epsilon), \tag{A.18}$$

where $\mathcal{H}'$ is the Hilbert transformation with respect to ξ'. Note that the sign in front of the Hilbert transformation is negative (when the infinitely deep fluid layer is in the lower side, the negative sign does not appear in front of the Hilbert transformation).

η' and ϕ'_2 are expanded in ϵ as follows:

$$\eta' = \eta'^{(0)} + \epsilon\eta'^{(1)} + \epsilon^2\eta'^{(2)} + \cdots, \tag{A.19a}$$

$$\phi'_2 = \phi'^{(0)}_2 + \epsilon\phi'^{(1)}_2 + \epsilon^2\phi'^{(2)}_2 + \cdots, \tag{A.19b}$$

so that

$$\phi'^{(0)}_2\big|_{Z'=\epsilon^2\eta'(\xi',y',t')} = -\mathcal{H}'\left\{\eta'^{(0)}\left(\xi', y', t'\right)\right\}. \tag{A.20}$$

Let us substitute (A.10) and (A.19a) in (A.7c) and collect the leading-order terms to obtain

$$-V_0^2\theta'^{(0)}_{\xi'} + (1 - R)\,\eta'^{(0)} = 0. \tag{A.21}$$

Then, the following equivalent expression arises in the leading order of (A.7a):

$$-\eta'^{(0)}_{\xi'} + H\theta'^{(0)}_{\xi'\xi'} = 0. \tag{A.22}$$

The next-order terms of $O(\epsilon^3)$ in (A.7a) read

$$- \eta'^{(1)}_{\xi'} + \eta'^{(0)}_{t'} + \theta'^{(0)}_{\xi'}\eta'^{(0)}_{\xi'} + \eta'^{(0)}\theta'^{(0)}_{\xi'\xi'} + H\theta'^{(1)}_{\xi'\xi'} + H\theta'^{(0)}_{y'y'} = 0, \tag{A.23}$$

where the last three terms come from $-\phi'_{1,z}$. Both $\theta'^{(0)}_{\xi'}$ and $\theta'^{(0)}_{\xi'\xi'}$ are eliminated from (A.23) by using (A.21) or (A.22), so that we have

$$- \eta'^{(1)}_{\xi'} + \eta'^{(0)}_{t'} + \frac{2}{H}\eta'^{(0)}\eta'^{(0)}_{\xi'} + H\theta'^{(1)}_{\xi'\xi'} + H\theta'^{(0)}_{y'y'} = 0. \tag{A.24}$$

Recalling that $V_0^2 = (1-R)H = O(\epsilon)$, from (A.10), (A.19), and (A.20), correct up to $O(\epsilon^3)$ in (A.7c), we have

$$- V_0^2\theta'^{(1)}_{\xi'} - RV_0^2\mathcal{H}'\{\eta'^{(0)}_{\xi'}\} + V_0^2\theta'^{(0)}_{t'} + (1-R)\eta'^{(1)} + \frac{1}{2}V_0^2\theta'^{(0)2}_{\xi'} - \epsilon\eta'^{(0)}_{\xi'\xi'} = O(\epsilon). \tag{A.25}$$

By taking differentiation with respect to ξ', we collect the leading-order terms in (A.25) by the virtue of (3.1) and (A.21) or (A.22) as follows:

$$- H\theta'^{(1)}_{\xi'\xi'} - RH\mathcal{H}'\{\eta'^{(0)}_{\xi'\xi'}\} + \eta'^{(0)}_{t'} + \eta'^{(1)}_{\xi'} + \frac{1}{H}\eta'^{(0)}\eta'^{(0)}_{\xi'} - \frac{\epsilon}{1-R}\eta'^{(0)}_{\xi'\xi'\xi'} = O(\epsilon) \tag{A.26}$$

since $V_0^2 \sim 1 - R \sim O(\epsilon)$. By adding (A.24) and (A.26) and then differentiating in ξ', both $\eta'^{(1)}_{\xi'}$ and $\theta'^{(1)}_{\xi'\xi'}$ are canceled out.

Finally, from (A.21) or (A.22) again, we end up with

$$\eta'^{(0)}_{t'\xi'} + \frac{3}{4H}\left(\eta'^{(0)}\right)^2_{\xi'\xi'} - \frac{RH}{2}\mathcal{H}'\{\eta'^{(0)}_{\xi'\xi'\xi'}\} - \frac{\epsilon}{2(1-R)}\eta'^{(0)}_{\xi'\xi'\xi'\xi'} + \frac{1}{2}\eta'^{(0)}_{y'y'} = O(\epsilon). \tag{A.27}$$

And then, the following two-dimensional model equation,

$$\frac{1}{V_0}\eta_{tx} + \eta_{xx} + \frac{3}{4H}\left(\eta^2\right)_{xx} - \frac{RH}{2}\mathcal{H}\{\eta_{xxx}\} - \frac{1}{2(1-R)}\eta_{xxxx} + \frac{1}{2}\eta_{yy} = 0, \tag{A.28}$$

is obtained by converting back to the original nondimensional variables through

$$\frac{\partial}{\partial t'} = \frac{\epsilon^{-2}}{V_0}\left(\frac{\partial}{\partial t} + V_0\frac{\partial}{\partial x}\right), \tag{A.29a}$$

$$\frac{\partial}{\partial \xi'} = \epsilon^{-1}\frac{\partial}{\partial x}, \tag{A.29b}$$

$$\frac{\partial}{\partial y'} = \epsilon^{-\frac{3}{2}}\frac{\partial}{\partial y}, \tag{A.29c}$$

$$\mathcal{H}'\{f(\epsilon s)\}(\xi') = \mathcal{H}\{f(s)\}(x), \tag{A.29d}$$

$$\eta'^{(0)} = \epsilon^{-1}\eta + O(\epsilon). \tag{A.29e}$$

Without the dependence on y', (A.28) is nothing but (3.2). This two-dimensional Benjamin equation, presented as 2-DB with different nondimensionalization in [14], involves the KP-I type transverse dispersion to the one-dimensional Benjamin (1-DB) equation.

Note that the coefficients of the linear terms agree with (A.1) and (A.2). The sign of the nonlinear coefficient is positive in this configuration. However, for the latter configuration where the finite-depth layer is on top, the sign of the coefficient of the nonlinear term should flip to be negative, without changing the magnitude. The signs of the coefficients in front of the Hilbert transformation, which accounts for the gravity term, and the third-order capillary term remain unchanged in either configuration. Therefore, the corresponding weakly nonlinear long-wave one-dimensional model equation for the latter configuration is finally given by

$$\sqrt{\frac{R}{(1-R)H}}\eta_t + \eta_x - \frac{3}{4H}\left(\eta^2\right)_x - \frac{H}{2R}\mathcal{H}\{\eta_{xx}\} - \frac{1}{2(1-R)}\eta_{xxx} = 0. \tag{A.30}$$

The associated two-dimensional model equation is obtained in the essentially same way as (A.28).

B. Estimation of the two potential functions

Under the assumption that the values of the two densities are close to each other and that the y-directional variation of the interfacial elevation is much more slowly varying than the x-directional one, the two potential functions are expressed in terms of the weakly nonlinear interfacial elevation.

From (A.5), (A.10), (A.21), and (A.29),

$$\theta'^{(0)}(\xi', y', t') = \frac{1}{H} \int_{-\infty}^{\xi'} \eta'^{(0)}(s', y', t')\mathrm{d}s', \tag{B.1}$$

and thus,

$$\phi_1(x, y, z, t) = \sqrt{\frac{1-R}{H}} \left\{ \int_{-\infty}^{x} \eta(s, y, t)\mathrm{d}s - \frac{1}{2}(z+H)^2 \eta_x(x, y, t) \right\} + O(\epsilon) \tag{B.2}$$

for $-H < z < \eta(x, y, t)$. From (A.5), (A.13), and (A.17), for the upper-layer potential, we obtain that

$$\phi_2(x, y, z, t) = V_0 \mathcal{F}^{-1} \left\{ \mathrm{i}\,\mathrm{sign}(k)\mathrm{e}^{-kz}\mathcal{F}\left\{\eta(x, y, t)\right\}(k) \right\} + O(\epsilon^2) \tag{B.3}$$

for $\eta(x, y, t) < z < +\infty$.

The expressions (B.2) and (B.3) support the statements on the circulation (4.2) and (4.3) in the Discussion.

References

1. Benjamin TB (1992) A new kind of solitary wave. J Fluid Mech 245:401–411
2. Benjamin TB (1967) Internal waves of permanent form in fluids of great depth. J Fluid Mech 29:559–592
3. Longuet-Higgins MS (1993) Capillary–gravity waves of solitary type and envelope solitons on deep water. J Fluid Mech 252:703–711
4. Akylas TR (1993) Envelope solitons with stationary crests. Phys Fluids 5:789–791
5. Dias F, Iooss G (1993) Capillary–gravity solitary waves with damped oscillations. Physica D 65:399–423
6. Longuet-Higgins MS (1989) Capillary–gravity waves of solitary type on deep water. J Fluid Mech 200:451–470
7. Vanden-Broeck J-M, Dias F (1992) Gravity–capillary solitary waves in water of infinite depth and related free-surface flows. J Fluid Mech 240:549–557
8. Dias F, Menasce D, Vanden-Broeck J-M (1996) Numerical study of capillary–gravity solitary waves. Eur J Mech B Fluid 15:17–36
9. Laget O, Dias F (1997) Numerical computation of capillary–gravity interfacial solitary waves. J Fluid Mech 349:221–251
10. Albert JP, Bona JL, Restrepo JM (1999) Solitary-wave solutions of the Benjamin equation. SIAM J Appl Math 59:2139–2161
11. Calvo DC, Akylas TR (2002) Stability of steep gravity–capillary solitary waves in deep water. J Fluid Mech 452:123–143
12. Calvo DC, Akylas TR (2003) On interfacial gravity–capillary solitary waves of the Benjamin type and their stability. Phys Fluids 15:1261–1270
13. Kataoka T (2008) Transverse instability of interfacial solitary waves. J Fluid Mech 611:255–282
14. Kim B, Akylas TR (2006) On gravity–capillary lumps. Part 2. Two-dimensional Benjamin equation. J Fluid Mech 557:237–256
15. Kim B, Akylas TR (2007) Transverse instability of gravity–capillary solitary waves. J Eng Math 58:167–175
16. Kalisch H (2007) Derivation and comparison of model equations for interfacial capillary–gravity waves in deep water. Math Comput Simul 74:168–178
17. Kataoka T, Tsutahara M (2004) Transverse instability of surface solitary waves. J Fluid Mech 512:211–221
18. Kataoka T (2006) The stability of finite-amplitude interfacial solitary wave. Fluid Dyn Res 38:831–867
19. Milewski PA (2005) Three-dimensional localized solitary gravity–capillary waves. Commun Math Sci 3:89–99
20. Parau E, Vanden-Broeck J-M, Cooker MJ (2005) Nonlinear three-dimensional gravity–capillary solitary waves. J Fluid Mech 536:99–105
21. Parau E, Vanden-Broeck J-M, Cooker MJ (2005) Three-dimensional gravity–capillary solitary waves in water of finite depth and related problems. Phys Fluids 17:122101

22. Kim B, Akylas TR (2005) On gravity–capillary lumps. J Fluid Mech 540:337–351
23. Akers B, Milewski PA (2009) A model equation for wavepacket solitary waves arising from capillary–gravity flows (preprint)
24. Akylas TR, Cho Y (2008) On the stability of lumps and wave collapse in water waves. Philos Trans R Soc Lond A 366:2761–2774
25. Ablowitz MJ, Segur H (1979) On the evolution of packets of water waves. J Fluid Mech 92:691–715
26. Djordjevic VD, Redekopp LG (1977) On two-dimensional packets of capillary–gravity waves. J Fluid Mech 79:703–714
27. Parau E, Vanden-Broeck J-M, Cooker MJ (2007) Three-dimensional gravity and gravity–capillary interfacial flows. Math Comput Simul 74:105–112
28. Parau E, Vanden-Broeck J-M, Cooker MJ (2007) Nonlinear three-dimensional interfacial flows with a free surface. J Fluid Mech 591:481–494
29. Agafontsev DS, Dias F, Kuznetsov EA (2006) Bifurcations and stability of internal solitary waves. JETP Lett 83:201–205
30. Agafontsev DS, Dias F, Kuznetsov EA (2007) Deep-water internal solitary waves near critical density ratio. Physica D 225:153–168
31. Barros R, Gavrilyuk S (2007) Dispersive nonlinear waves in two-layer flows with free surface part II. Large amplitude solitary waves embedded into the continuous spectrum. Stud Appl Math 119:213–251
32. Dias F, Iooss G (2003) Water-waves as a spatial dynamical system. In: Friedlander S, Serre D (eds) Handbook of mathematical fluid dynamics. Elsevier, Amsterdam pp 443–499
33. Bridges TJ (2001) Transverse instability of solitary-wave states of the water-wave problem. J Fluid Mech 439:255–278
34. Tanaka M (1986) The stability of solitary waves. Phys Fluids 29:650–655
35. Longuet-Higgins MS (1974) On the mass, momentum, energy and circulation of a solitary wave. Proc R Soc Lond A 337:1–13
36. Groves MD, Sun S-M (2008) Fully localised solitary-wave solutions on the three-dimensional gravity–capillary water-wave problem. Arch Ration Mech Anal 188:1–91
37. Rousset F, Tzvetkov N (2008) Transverse nonlinear instability of solitary waves for some Hamiltonian PDE's. J Math Pure Appl 90:550–590